Brain Structure and Function (2020) 225:441–459
https://doi.org/10.1007/s00429-019-02002-8

ORIGINAL ARTICLE

Structural abnormalities in thalamo-prefrontal tracks revealed by high angular resolution diffusion imaging predict working memory scores in concussed children

Guido I. Guberman[1,4] · Jean-Christophe Houde[2] · Alain Ptito[1] · Isabelle Gagnon[3] · Maxime Descoteaux[2]

Received: 10 May 2019 / Accepted: 5 December 2019 / Published online: 1 January 2020

Abstract

Because of their high prevalence, heterogeneous clinical presentation, and wide-ranging sequelae, concussions are a challenging neurological condition, especially in children. Shearing forces transmitted across the brain during concussions often result in white matter damage. The neuropathological impact of concussions has been discerned from animal studies and includes inflammation, demyelination, and axonal loss. These pathologies can overlap during the sub-acute stage of recovery. However, due to the challenges of accurately modeling complex white matter structure, these neuropathologies have not yet been differentiated in children in vivo. In the present study, we leveraged recent advances in diffusion imaging modeling, tractography, and tractometry to better understand the neuropathology underlying working memory problems in concussion. Studying a sample of 16 concussed and 46 healthy youths, we used novel tractography methods to isolate 11 working memory tracks. Along these tracks, we measured fractional anisotropy, diffusivities, track volume, apparent fiber density, and free water fraction. In three tracks connecting the right thalamus to the right dorsolateral prefrontal cortex (DLPFC), we found microstructural differences suggestive of myelin alterations. In another track connecting the left anterior-cingulate cortex with the left DLPFC, we found microstructural changes suggestive of axonal loss. Structural differences and tractography reconstructions were reproduced using test–retest analyses. White matter structure in the three thalamo-prefrontal tracks, but not the cingulo-prefrontal track, appeared to play a key role in working memory function. The present results improve understanding of working memory neuropathology in concussions, which constitutes an important step toward developing neuropathologically informed biomarkers of concussion in children.

Keywords Concussion · Mild TBI · Diffusion-weighted imaging · Constrained spherical deconvolution

Introduction

Traumatic brain injury (TBI) is common, affecting up to 600 per 100,000 individuals (Cassidy et al. 2004). The highest incidence rate occurs in early childhood and late adolescence (Faul et al. 2010). Its effect is wide ranging, negatively impacting memory, mood, cognition, behavior, and brain aging (Carroll et al. 2004; Dean et al. 2012; Kristman et al. 2014; Landre et al. 2006; McKee et al. 2009; Orlovska et al. 2014; Spinos et al. 2010). Mild forms of TBI (mTBIs or concussions, used here interchangeably) are the most common (Peeters et al. 2015) and are generally undetectable by conventional imaging such as computerized tomography (Lewine et al. 1999; Shenton et al. 2012; Sundman et al. 2015; Yuh et al. 2013) to the extent that cases of mTBI can often go undiagnosed (Meehan et al. 2013; Yuh et al. 2013). In cases of subtle or subclinical brain injuries, youths could

Electronic supplementary material The online version of this article (https://doi.org/10.1007/s00429-019-02002-8) contains supplementary material, which is available to authorized users.

✉ Guido I. Guberman
guido.guberman@mail.mcgill.ca

1 Department of Neurology and Neurosurgery, Faculty of Medicine, McGill University, Montreal, QC, Canada

2 Department of Computer Science, Sherbrooke University, Sherbrooke, QC, Canada

3 Department of Pediatrics, Faculty of Medicine, Montreal Children's Hospital, McGill University, Quebec, Canada

4 Montreal Neurological Institute, 3801 University, Montreal, QC H3A 2B4, Canada

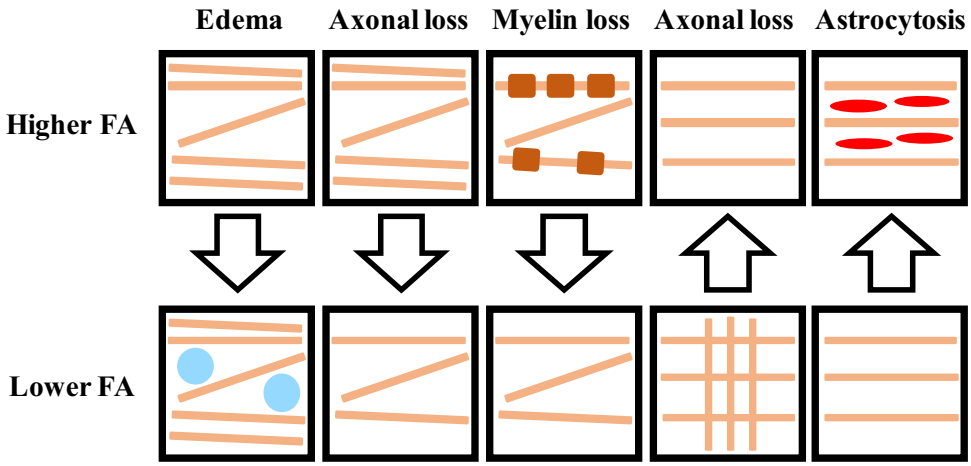

Fig. 1 Conceptualized illustration of the relative degree of FA in the context of different neuropathological processes. Arrows denote the direction of change as a result of injury

be prematurely cleared to return to activities of daily life in the presence of incomplete cerebral recovery (Churchill et al. 2017) with potentially devastating consequences. Further, far fewer biomarker studies exist in children than in adults (Mayer et al. 2018). Neuroimaging biomarkers for pediatric concussions are still needed.

During a concussive event, the brain's white matter tends to be heavily affected (Bigler and Maxwell 2012; Hayes et al. 2016). Diffusion-tensor imaging (DTI) provides metrics that describe water diffusion such as fractional anisotropy (FA), axial diffusivity (AD), mean diffusivity (MD), and radial diffusivity (RD). These measurements are used to infer properties of white matter structure. A review of 100 DTI studies of TBI found that the vast majority of articles reported decreases in FA in injured individuals (Hulkower et al. 2013). Further, in a longitudinal study of 27 concussed varsity athletes, Churchill et al. (2017) found acute decreases in FA which remained present when patients were cleared to return to play. Hence, on long timescales, FA measurements can reliably detect abnormalities, even in the absence of symptoms.

Work from animal models has shown that shortly after impact, the affected brain areas can display an edematous inflammatory response, accompanied by blood flow alterations, as well as metabolic abnormalities (Bigler and Maxwell 2012). On longer timescales, as a result of these processes or in parallel, chronic neuroinflammation and edema, axonal demyelination, and/or axonal death can occur (Bigler and Maxwell 2012; Pasternak et al. 2016). A DTI study using a mouse model of traumatic axonal injury showed that the presence of edema reduces FA (Mac Donald et al. 2007), which is known to result from an increase in free water (Pasternak et al. 2016). By decreasing diffusion hindrance, demyelination decreases FA (Budde et al. 2011) and so does loss of axons (Harsan et al. 2006; Sun et al. 2006). However, in voxels with crossing fibers, loss of axons in one fiber population can paradoxically lead to an increase in FA (Douaud et al. 2011; Pierpaoli et al. 2001). During recovery, coherent astrocyte reactivity can also increase FA (Budde et al. 2011). Given its low specificity (Fig. 1), FA cannot disambiguate between these different pathologies. As a result, individuals undergoing recovery at different rates can give rise to conflicting patterns of FA change across groups of concussed patients. A recent review, focused on patients in sub-acute stages of recovery (approximately, 3 months), found, contrary to Hulkower et al. (2013), mixed results regarding the direction of FA change (Dodd et al. 2014). Disambiguating the different forms of neuropathology present in patients at the sub-acute phase is therefore still needed given that each may have different clinical outcomes and require distinct treatment approaches.

Using other tensor-based measures has been proposed to complement FA and provide more information about mTBI neuropathology (Bigler and Maxwell 2012; Budde et al. 2011). For instance, demyelination has been shown to increase RD and MD (Budde et al. 2011), whereas with loss of axons, a decrease in AD can be observed (Harsan et al. 2006; Sun et al. 2006). Despite these findings, interpretations of white matter microstructure from tensor-based measurements are limited (Jones et al. 2013), given that DTI assumes a single predominant fiber orientation per voxel (Tournier et al. 2008). Recent work suggests that this assumption is inaccurate across the majority of white matter voxels (Jeurissen et al. 2013).

In the present study, we used advances in high angular resolution diffusion imaging (HARDI) local modeling, tractography, and tractometry to improve understanding of the neuropathology involved in concussion by using measures that, individually or in combination, provide information that is more specifically related to particular neuropathological processes. Given the wide scope of this question, we decided to focus on working memory deficits, a well-studied post-concussive abnormality. Previous work has repeatedly shown that concussed children and adults performing

working memory tests display altered brain activity in the dorsolateral prefrontal cortex (DLPFC) as well as in other areas of the brain, irrespective of test performance (Chen et al. 2007, 2004; Jantzen et al. 2004; Keightley et al. 2014; McAllister et al. 1999, 2001; Pardini et al. 2010; Westfall et al. 2015). The areas of the brain related to working memory are well known, and focusing on this phenomenon allowed us to hone in on a small subset of 11 reliable tracks.[1] Microstructural differences at the whole-track and segment level were found for three right thalamo-prefrontal and one left cingulo-prefrontal tracks, suggestive of different, concurrent neuropathological processes. These differences were replicated in test–retest analyses using a second set of scans available for most participants. White matter structure in the thalamo-prefrontal tracks appeared to play a key role in working memory deficits in concussion.

Materials and methods

Sample

Participants included 20 youths (11 females, 9 males; mean age = 14.36 years, SD = 2.65) who had previously sustained a concussion ranging from 9 to 96 days at the time of testing (Table 2). Data from a group of 51 (20 females, 31 males, mean age = 15.09, SD = 1.89) healthy controls were obtained from previous imaging studies at the Montreal Neurological Institute. Patients were included in the study if they had received a diagnosis of mTBI, as per the World Health Organization task force definition (Cassidy et al. 2004) by a physician at the Montreal Children's Hospital Concussion Clinic (Montreal, Quebec, Canada). All participants were screened prior to testing for a history of concussion, as well as to rule out other neurological conditions, including learning disabilities and ADHD. Participants were also excluded if they reported vestibular or musculoskeletal problems (other than upper extremity injuries), and if they had any contraindications for MRI, such as claustrophobia or metallic implants. Control participants had the same inclusion and exclusion criteria except for the additional restriction of not having sustained any previous concussions. Further information on recruitment and operational criteria for the identification of concussion are outlined in Keightley et al. (2014). No participants had abnormalities on standard imaging. Every participant provided informed written consent as approved by the ethics committee at McGill University, Montreal Neurological Institute.

[1] Throughout the manuscript we refer to real white matter bundles as "tracts", and reconstructions of those tracts from tractography as "tracks".

Neuropsychological testing

All participants completed a verbal and visual working memory test which consisted of an adapted version of the externally ordered working memory task, described elsewhere (Petrides et al. 2001). This task consists in having participants familiarize with a set of five items (pseudo words for verbal, abstract drawings for visual). On each trial, four of the five items were randomly chosen and presented in succession, in random order. After the fourth item was presented, a 1 s delay occurred. After this delay, a test item was presented. Participants had to answer Yes or No to whether the item that was presented was one of the four items presented before the delay. This task has been validated in studies of patients and non-human primates with lateral prefrontal lesions (Petrides et al. 1993; Stern et al. 2000) and has been used in both concussed adults (Chen et al. 2004) and children to demonstrate reduced DLPFC activation, including in a subset of the present sample (Keightley et al. 2014). All participants also filled out a 22-item adapted version of the post-concussion symptom scale (Lovell et al. 2006).

Imaging acquisition

All HARDI scans were acquired at the Montreal Neurological Institute using a 3.0 T Siemens MAGNETOM Trio A Tim System with a 32-channel head coil. Each session started with acquisition of a high-resolution T1-weighted 3D anatomical image using 3D magnetization prepared rapid gradient echo (MP-RAGE) sequence (TR = 23 ms, TE = 2.98 ms, slice thickness = 1 mm, image matrix = 256 × 256, flip angle = 9°, FOV = 256 mm, interleaved excitation). DWI data were acquired with the following parameters: TR = 8300 ms, echo time: 88 ms, slice thickness = 2 mm, FoV = 256 mm, matrix = 128 × 128, number of slices = 64, interleave excitation. Diffusion weighting was performed along 99 non-collinear directions using a b-value of 1000 s/mm^2. Ten b = 0 s/mm^2 images were acquired as reference. Out of 71 subjects, 67 underwent 2 DWI scans. All main analyses were performed on run 1 data. Run 2 data were used for replication purposes.

Processing

A rigorous quality assessment procedure (see Supplementary Material) was performed by an experienced visual rater (GIG) to flag images that had severe artifacts that can affect DWI metrics (Tournier et al. 2011). Only images that passed were processed. Except where otherwise indicated, all steps in the processing pipeline were performed using the Diffusion Imaging for Python (DIPY) library and scripts built on it (Garyfallidis et al. 2014) (https://github.com/scilus/scilpy/). Images were first brain extracted using FSL's *BET*

command (Smith 2002; Woolrich et al. 2009) and then de-noised using Non-Local Spatial and Angular Matching, a novel tool that can be applied to any existing data and which improves the visual quality of data and results in more accurate and reproducible tractography results (St-Jean et al. 2016). Images were then corrected for magnetic field inhomogeneity using advanced normalization tools (ANTs) (Avants et al. 2011) and then eddy current and motion corrected using FSL's *eddy* command (Andersson and Sotiropoulos 2016). Lastly, DWI images were upsampled to $1 \times 1 \times 1$ space using trilinear interpolation (Girard et al. 2014; Tournier et al. 2012), a procedure that, when performed before tractography, increases anatomical contrast, reduces partial volume effects and yields more accurate tract reconstructions (Dyrby et al. 2014).

Local modeling

Free-water modeling was performed using the accelerated microstructure imaging via convex optimization (AMICO) (Daducci et al. 2015) to calculate free-water fraction (FW), which is thought to be related to neuroinflammation (Pasternak et al. 2016, 2012, 2009). The processed DWI images were then corrected for FW, and water diffusion was modeled on FW-corrected DWI images at each voxel using a tensor, creating maps of FW-corrected tensor metrics (FA, AD, MD, and RD). Outliers were then removed from FW-corrected AD, RD, and MD maps. Recent work suggests that removing outliers increases the robustness of tensor-based measurements (Jones et al. 2013). Then, fiber orientation distribution functions (fODFs) were computed using constrained spherical deconvolution (CSD) (Descoteaux et al. 2009; Tournier et al. 2007). Since fiber response functions (FRF) did not differ between groups, CSD was performed using an FRF averaged across all participants (Mito et al. 2018; Pierpaoli and Basser 1996).

Tractography

Probabilistic tractography was performed in upsampled DWI space using particle filtering tractography (PFT) with anatomical priors. This method consists in optimizing tractography parameters by informing stopping criteria using partial volume estimation maps computed from high-resolution T1-weighted images which were transformed to upsampled DWI space using ANTs symmetric normalization (SyN) algorithm (Avants et al. 2008, 2011). These maps provide an anatomically informed, probabilistic stopping criterion, which, combined with a particle filtering method, can achieve tractography results that are less biased by length, shape, size, and position (Girard et al. 2014). The anatomical constraints used in this algorithm are: (1) the initiation of streamlines from the gray/white matter interface; and (2) the obligatory termination of streamlines in gray matter. Gray/white matter interface maps were created using FSL's FAST (Zhang et al. 2001) in the transformed T1-weighted images. Seeding along the interface maps was performed using 24 seeds per voxel, which yielded an average of 2.3 million streamlines ($SD = 7.58 \times 10^5$). Tractograms were cleaned by removing loops (defined as streamlines with angles above 330°).

Track selection

The full track selection procedure is illustrated in Fig. 2. To select tracks for tractometry analyses, connectivity matrices were first created using the Brainnetome Atlas, a connectivity-based parcellation with 210 cortical and 36 subcortical labels (Fan et al. 2016). For each subject, a 1 mm MNI-152 template (Maintz and Viergever 1998) was warped onto upsampled DWI space using ANTs SyN algorithm. The Brainnetome Atlas is freely available (https://atlas.brainnetome.org/download.html) in MNI-152 space. The resulting transformations from the SyN algorithm were used to convert Brainnetome parcellations onto the upsampled DWI space. Using DIPY, a connectivity matrix detailing the number of streamlines connecting each pair of labels was computed (Fig. 2a). All streamline counts were normalized by the total amount of streamlines for each subject. The matrices of normalized streamline counts were then binarized using a threshold of at least one streamline (Fig. 2b).

In the present study, we were interested in tracks connecting the DLPFC with other areas of the brain involved in working memory. Given that Brainnetome does not contain a DLPFC label, we first defined the DLPFC using six labels (Table 1 and Table S1). Next, we defined other regions involved in working memory using 30 labels (Table 1 and Table S1). All labels were selected based on previous literature (Keightley et al. 2014). Tracks that connected one of six DLPFC labels with one of 30 working memory labels were isolated (Table 1 and Fig. 2b). Then, only tracks defined by a working memory label that had an existing connection with a DLPFC label across all 62 subjects were selected for tractometry analyses (Fig. 2c). This strict, functionally informed procedure yielded 11 reliable tracks (see Fig. 3).

Tractometry

After selecting a reliable set of tracks, we proceeded with a two-stage track-of-interest analysis. First, the following measurements were taken across the entire track (Fig. 2d): normalized streamline count, normalized track volume, FW, apparent fiber density (AFD), and FW-corrected FA, AD, MD, and RD. FW and all FW-corrected tensor-based metrics were extracted from voxel-level measurements, whereas AFD was calculated along streamlines, at the

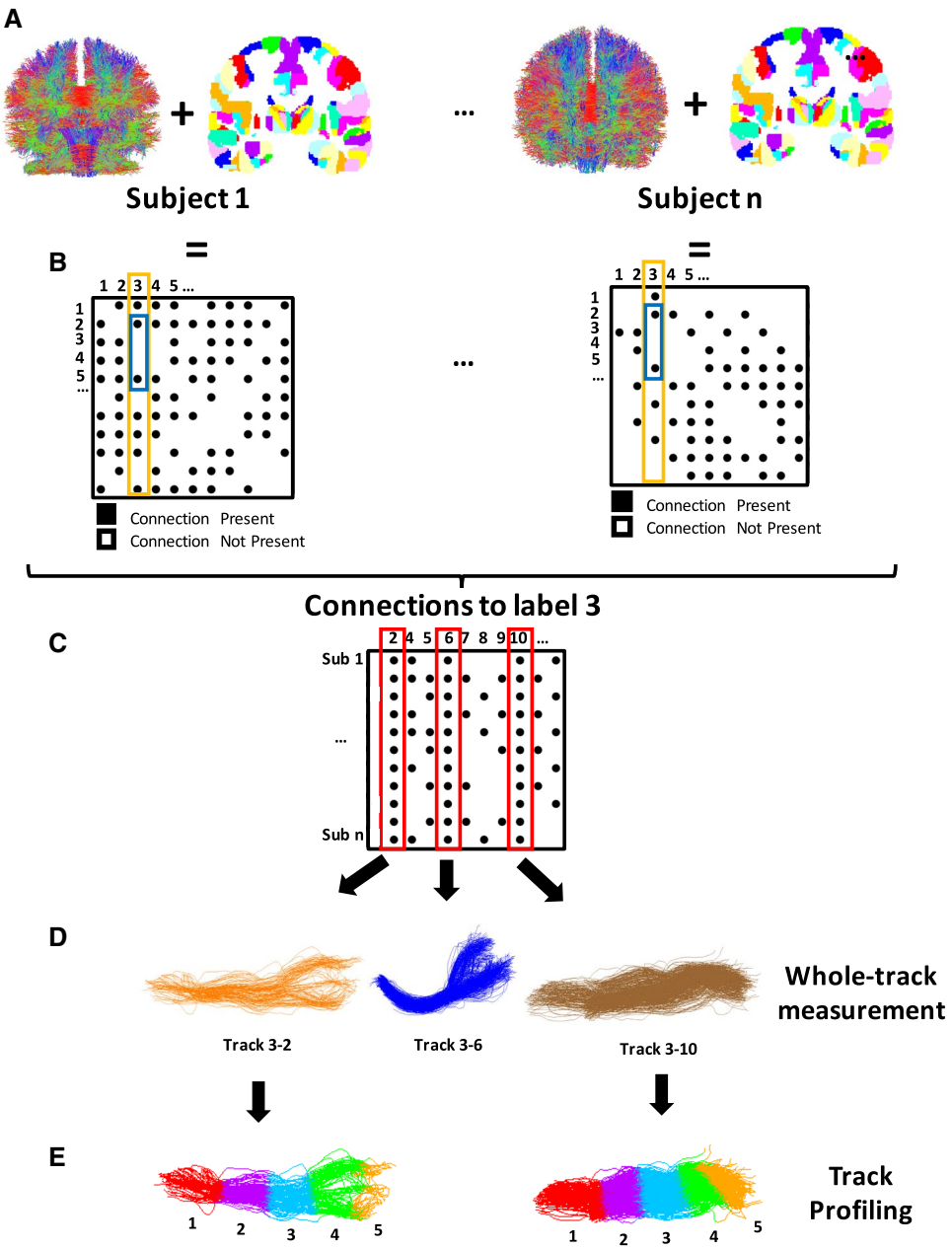

Fig. 2 Illustration of the track selection and tractometry methodology. **a** Connectomes were built by first segmenting individual whole-brain tractograms using a Brainnetome parcellation (Fan et al. 2016) that was transformed to upsampled DWI space using ANTs. **b** Connectomes were binarized such that pairs of regions with at least one streamline were assigned a value of 1, and otherwise a value of 0. Labels corresponding to DLPFC regions were selected from binarized connectomes (yellow rectangle), and connections of the DLPFC with other working memory regions were then selected (blue rectangle). **c** Matrices containing binarized connectivity values were built for each DLPFC region. These matrices contained all working memory regions selected in the previous step for all subjects. Tracks defined by pairs of regions with an existing connection across all subjects were selected (red rectangle). **d** For each selected track, normalized streamline count, normalized track volume, AFD, FW, and FW-corrected FA, AD, MD, and RD were measured across the entire track. **e** Tracks in which differences were found underwent track profiling. Tracks were divided into five segments, and the values of AFD, FW, and FW-corrected FA, AD, MD, and RD were measured at each segment

intra-voxel level (Raffelt et al. 2017). Track volumes were normalized by total brain volume. All measurements were weighted by streamline density to minimize the impact of spurious streamlines.

Second, tracks that displayed a significant difference in the first stage were divided into five segments (Fig. 2E). The following measurements were taken at each segment to create track profiles: FW-corrected FA, AD, MD, RD, as well as AFD and FW. Track profiling was used because it has been shown to be more sensitive than whole-track measurements at detecting subtle changes which correlate well with behavior (Yeatman et al. 2012). In follow-up analyses, the number of fiber orientations (NuFO) (Dell'Acqua et al. 2013) was also measured.

Statistical analyses

Skewness and kurtosis analyses of whole-track measurements show that streamline count measures were not normally distributed. Hence, group comparisons were performed using rank-sum tests on Matlab (Version R2018b), and except where otherwise indicated, group descriptive statistics are reported as medians. Given the known impact of neuropathological processes on diffusion measurements,

Table 1 Label numbers and names of end points of all studied tracks

DLPFC labels		Connected working memory areas[a]	
Label number	Label name[b]	Label number	Label name[b]
15	Left dorsal area 9/46	231	Left medial pre-frontal thalamus
16	Right dorsal area 9/46	138	Right inferior parietal lobule, rostrodorsal area 39
		140	Right inferior parietal lobule, rostrodorsal area 40
		232	Right medial pre-frontal thalamus
		234	Right pre-motor thalamus
		246	Right lateral pre-frontal thalamus
19	Left area 46	179	Left cingulate gyrus, pregenual area 32
		231	Left medial pre-frontal thalamus
21	Left ventral area 9/46	179	Left cingulate gyrus, pregenual area 32
22	Right ventral area 9/46	232	Right medial pre-frontal thalamus
		246	Right lateral pre-frontal thalamus

[a]Across 100% of subjects

[b]Anatomical and modified cyto-architectonic descriptions provided with the Brainnetome Atlas

the following hypotheses were posited. In relation to myelin loss, we hypothesized that FA would be lower in concussed individuals and RD and MD would be higher (Budde et al. 2011). In relation to axonal loss, we hypothesized that AFD and AD would be lower in concussed individuals (Harsan et al. 2006; Raffelt et al. 2012; Sun et al. 2006). In relation to edema, we hypothesized that FW would be higher in concussed individuals (Pasternak et al. 2016). Since the objective of the study is to detect these specific patterns of microstructural changes, one-tailed tests according to these hypotheses were used in group comparisons. Given that the direction of change in FA is equivocal (Dodd et al. 2014) in the sub-acute stage, group comparisons of FA, as well as any other comparisons not mentioned above, were performed using two-tailed tests. To assess the impact of microstructure on working memory accuracy, multiple linear regressions were performed using an ordinary least squares estimation method. Since several correlated variables were entered into the models, a backward elimination procedure was performed. This procedure consists in creating an initial model with all variables included, identifying variables with a p value above a pre-defined criterion ($p = 0.100$) and computing the model again after removing, from those identified variables, the one with the highest p value. This procedure was repeated until there were no more variables left to remove. These tracks were expected to be related to working memory irrespective of group, so the main regression models were computed using data from both groups. Regression coefficients are reported in scales that reflect group differences. Assumptions of final regression models were verified: normality (skewness, kurtosis, Normal P–P plots of standardized residuals), linearity, homoscedasticity (scatter plot of standardized residuals and standardized predicted values), independence (Durbin Watson d score of 0 or 4), outliers (z-scores higher than 4 or below − 4, and Cook's distance scores above 4) and multicollinearity (tolerance < 0.1, variance inflation factors > 10, and condition indices > 30). Regression models and assumption verifications were performed using IBM SPSS Statistics for MacIntosh, Version 25.0.

Data availability

Raw diffusion-weighted and T1-weighted images, as well as working memory scores for all participants, are available on Open Science Framework (Guberman 2019).

Results

Sample after QA

After QA, the selected sample for run 1 consisted of 62 subjects, 16 concussed (10 females, 6 males, mean age = 14.75, SD = 2.64) and 46 age- and sex-matched healthy controls (17 females, 29 males, mean age = 15.09, SD = 2.01). Time since injury for the selected concussed participants ranged from 9 to 96 days, with an average of 38.25 days. Despite being balanced for age (CC = 15.80; HC: 15.47; $W = 490$, $p = 0.83$) and sex (CC = 37.5% males, 62.5% females; HC: 63% males, 37% females; $\chi^2 = 3.15$, $p = 0.08$), groups were not balanced for handedness (CC: 62.5% right handed, 37.5% left handed; HC: 95.7% right handed, 4.3% left handed; $\chi^2 = 11.61$, $p < 0.001$). There were no significant differences in age between the included and the excluded participants (included = 15.59, excluded = 13.74, $W = 2306$, $p = 0.20$). Information on the mechanisms of injury for the included concussed participants is summarized in Table 2.

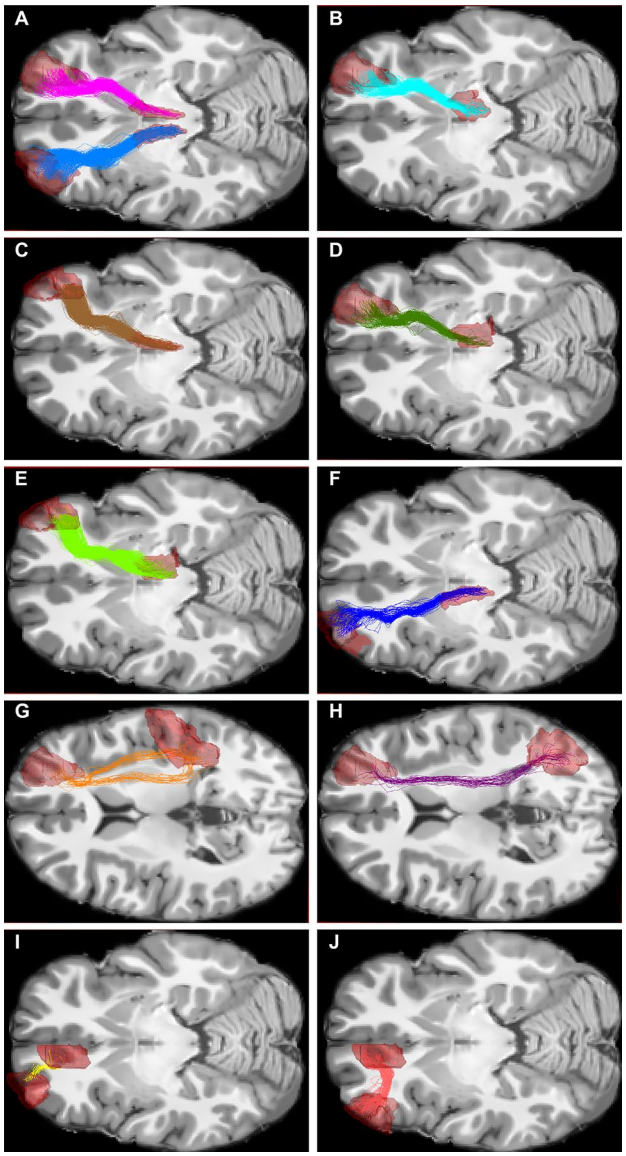

Fig. 3 Illustration of the 11 selected working memory tracks in one subject. End points (shown in red) are listed in Table 1. **a** Magenta: track 16-232; blue: track 15-231. **b** Track 16-234. **c** Track 22-232. **d** Track 16-246. **e** Track 22-246. **f** Track 19-231. **g** Track 16-140. **h** Track 16-138. **i** Track 19-179. **j** Track 21-179

Tractometry: whole track

Our track selection procedure yielded 11 tracks (Fig. 3). The labels that defined each track are outlined in Table 1. From these 11 tracks, two displayed differences in streamline count. Concussed youths had significantly lower streamline count than healthy controls in two thalamo-prefrontal tracks, track 16-246 (Fig. 4a, Table 3) and track 22-246 (Figure S1, Table S2). In track 22-246, concussed youths also had lower AD, higher MD, and higher RD (Table S2). Similar differences in AD, MD, and RD were found in another thalamo-prefrontal track, track 22-232, and a cingulo-prefrontal track, track 21-179. Lastly, concussed youths had significantly lower AFD than healthy controls across track 21-179 (Fig. 5a, Table 4). No significant differences in track volume, FA, or FW were apparent across whole tracks.

Tractometry: track profiling

Track profiles of FA, AD, MD, RD, AFD, and FW were created for tracks 16-246 (Fig. 4b, Table 3), 22-246 (Figure S1), 22-232, and 21-179 (Fig. 5b, Table 4). Concussed individuals had lower FA than healthy controls in segment 2 of track 16-246. In the same segment, concussed youths had lower AD, higher MD, higher RD, and higher FW than healthy controls. In segment 3 of track 16-246, concussed individuals also displayed lower AD, and higher MD and RD. Concussed individuals also had lower FA than healthy controls in segment 2 of track 22-246, as well as lower AD (Table S2). In the same segment, concussed individuals had higher MD and RD. In segment 3 of this same track, concussed individuals also had lower AD, and higher MD and RD. Concussed individuals also had lower FA than healthy controls in segment 2 of track 22-232, and lower AD. In the same segment, concussed individuals had higher MD and RD. In segment 3 of this same track, concussed individuals also had lower AD, and higher MD and RD (Table S3). Lastly, concussed individuals had lower AFD compared to healthy controls in segment 3 of track 21-179. In segment 2 of track 21-179, concussed individuals had lower AD and higher MD and RD.

Relation between white matter and working memory

Concussed youths had lower verbal (CC: 60, HC: 71; $W = 297$, $p = 0.001$) and visual working memory accuracy (CC: 58.5, HC: 72; $W = 269$, $p < 0.001$). To assess whether working memory was associated with white matter structure, linear regression analyses were computed using white matter measurements from all significant segments to predict verbal and visual working memory accuracy. Kurtosis and skewness were measured for all track profile variables that were significantly different between groups. Only one variable, FW in segment 2 of track 16-246, had kurtosis and skewness values suggesting non-normality. This variable was log transformed, which fixed its non-normality. Given that several highly correlated microstructural measurements were entered in the models, backward stepwise regressions were performed. Once a final set of predictors was obtained, assumptions of linear regression were verified. For track 16-246 (Fig. 6a), backward regression yielded a final model significantly predicting verbal working memory [$F(1,59) = 12.20$, $p = 0.001$], which accounted for 17% of

Table 2 Demographic characteristics of the concussed group

Subject ID	Gender	Age (years)	Time since injury (days)	Mechanism of injury	PCS	Number of previous concussions
TC079	F	10	41	Hit wall in gym class	2	0
TC033	M	12	92	Fell playing soccer	17	0
TC078	F	13	12	Fell playing ringette	57	0
TC050	M	11	50	Hit head while swimming	32	0
TC056	F	14	83	Hit head against wall while swimming	47	0
TC007	F	15	19	Hit in head by ball in soccer	45	1
TC074	F	15	35	Fell playing ringette	12	0
TC069	F	17	72	Hit in head by ball playing soccer	29	0
TC001	M	17	9	Fell while skiing	39	0
TC076	M	17	9	Hit head playing football	54	1
TC077	F	17	43	Hit head playing soccer	33	0
TC054	M	11	17	Ran into a door	28	0
TC057	F	11	9	Hit head on side of trampoline	39	0
TC042	F	16	96	Kneed in the head playing soccer	9	0
TC073	F	16	11	Fell while snowboarding	73	6
TC071	M	17	14	Fell while skiing	5	0

the variance and contained one significant factor. Participants' verbal working memory scores increased by 1.097 units for every 1×10^{-7} unit increase of AD in segment 2 of track 16-246. In addition, backward regression yielded a final model significantly predicting visual working memory [$F(1,59) = 10.43$, $p = 0.002$], which accounted for 15% of the variance and contained one significant factor. Participants' visual working memory scores decreased by 0.007 units for every 1×10^{-3}-unit increase in the log-transformed FW variable in segment 2 of track 16-246 (Fig. 5a). The results were similar for tracks 22-246 and 22-232 and are outlined in Supplementary Material.

Finally, for track 21-179 (Fig. 6b), backward regression yielded a final model that significantly predicted verbal working memory [$F(1,59) = 4.979$, $p = 0.029$], which accounted for 8% of the variance and contained one significant factor. Participants' verbal working memory accuracy scores increased 1.020 units for every increase in 1×10^{-7} units of AD in segment 2 of track 21-179. For visual working memory, backward regression yielded a final model that did not significantly predict verbal working memory [$F(1,59) = 3.505$, $p = 0.066$].

All assumptions of linear regressions—normality, linearity, homoscedasticity, independence, outliers, and multicollinearity—were verified in the final models and were found to be satisfied. These eight regression models were corrected for multiple comparisons. Using a Bonferroni correction, a more conservative threshold of $0.05/8 = 0.006$ was obtained. For track 16-246, AD of segment 2 retained significance, as well as log-transformed FW of segment 2. For both tracks 22-246 and 22-232, models predicting verbal working memory retained significance, whereas models predicting visual working memory did not. For track 21-179, AD of segment 2 did not survive Bonferroni correction.

Relation between white matter and concussion symptoms

The measures of track microstructure correlated with individual PCS scores in concussed participants (Table 5). In segment 2 of track 16-246, AD was significantly negatively correlated with remembering difficulties. In this same segment, log-transformed FW was significantly positively correlated with vomiting. In segment 2 of track 22-246, FA was significantly negatively correlated with nausea and nearly significantly correlated with remembering difficulties. In segment 2 of track 22-232, FA was significantly positively correlated with nausea and dizziness. Lastly, in segment 2 of track 21-179, AD was significantly negatively correlated with noise sensitivity and nearly significantly correlated with remembering difficulties. Other significant or nearly significant correlations are listed in Table 5. However, no tests survived a Benjamini–Hochberg false discovery rate (FDR) correction for multiple comparisons.

Follow-up analyses

Further analyses were performed to account for other potential factors that may have influenced the results.

Controlling for effect of group. We tested the impact of group (effects coded) as well as the interaction between group and the diffusion metrics (after centering) in each of

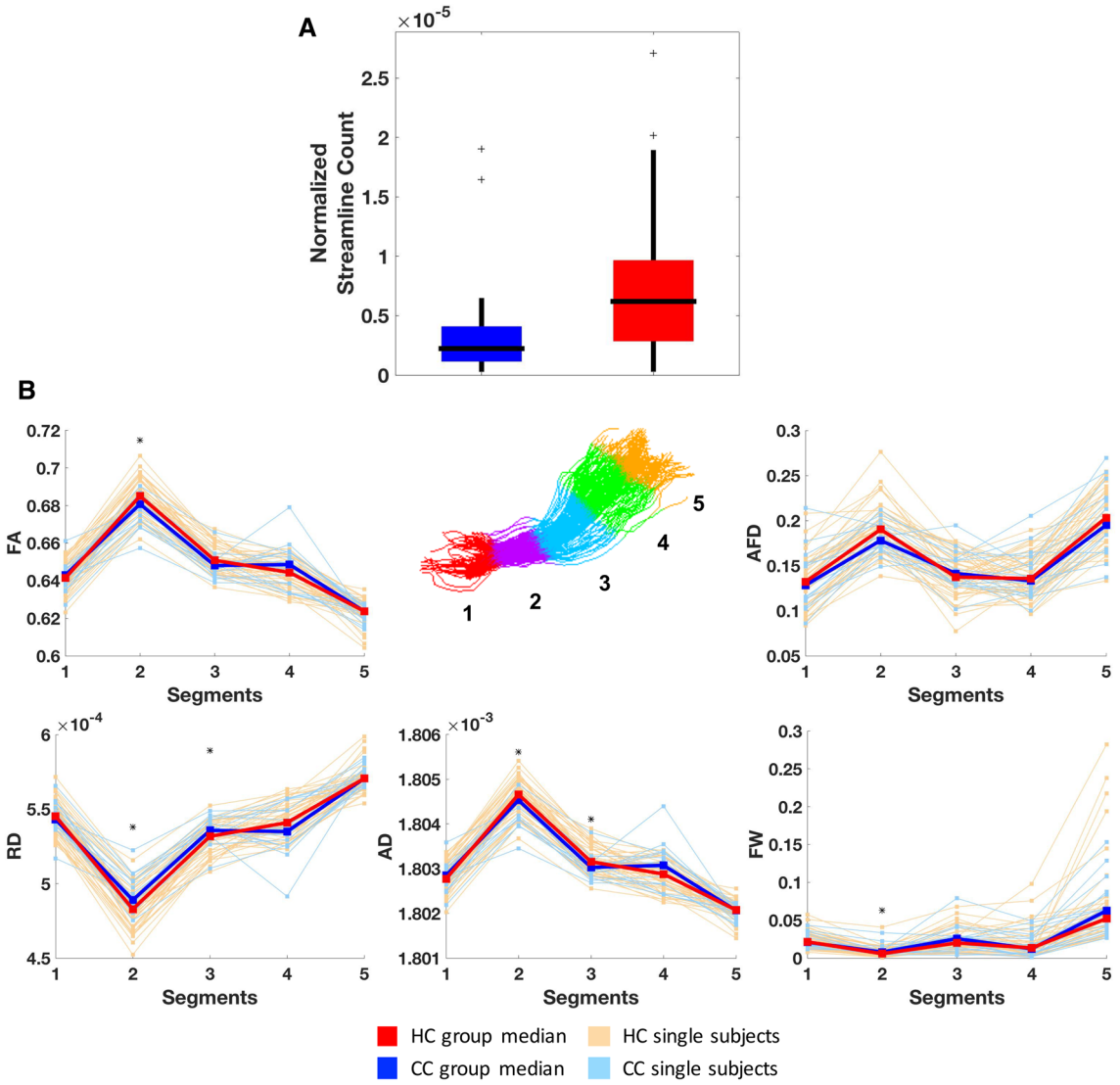

Fig. 4 Results of track 16-246. **a** Box plots comparing normalized streamline count between concussed (blue) and healthy control (red) groups. Horizontal black lines illustrate group medians, the edges of the boxes illustrate 75th (upper edge) and 25th (lower edge) percentiles, vertical black lines illustrate ranges, and black '+' signs illustrate outliers. **b** Line plots showing track profiles for AFD, FW, and FW-corrected FA, RD, and AD. Light red and light blue lines indicate median values of each segment for each individual healthy or concussed subject, respectively. Dark red and dark blue lines indicate instead group medians at each segment. *$p < 0.05$

Table 3 Results for track 16-246

Segment	Metric	Concussed	Healthy	Mann–Whitney	
				W	*p*
Whole track	Streamline count	0.223×10^{-5}	0.620×10^{-5}	346	0.011
2	AD	18.045×10^{-4}	18.047×10^{-4}	359	0.010
	FA	0.68	0.69	357	0.018
	MD	9.275×10^{-4}	9.234×10^{-4}	651	0.009
	RD	4.890×10^{-4}	4.828×10^{-4}	651	0.009
	FW	0.0079	0.0057	616	0.036
3	AD	18.030×10^{-4}	18.032×10^{-4}	387	0.031
	MD	9.581×10^{-4}	9.555×10^{-4}	614	0.039
	RD	5.357×10^{-4}	5.317×10^{-4}	614	0.039

Units of AD, MD, RD = mm^2/s. FW and FA have no units

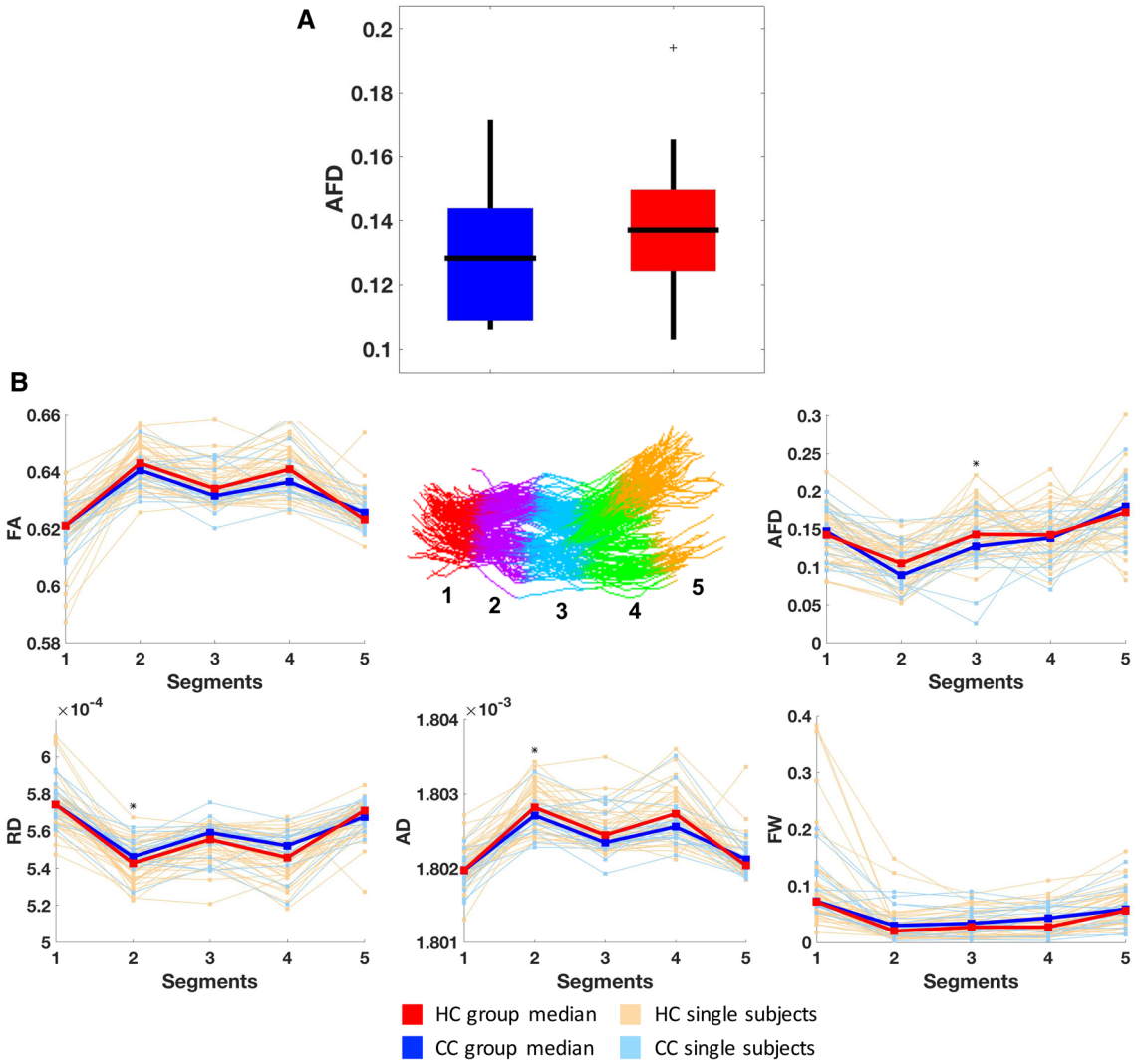

Fig. 5 Results of track 21-179. **a** Box plots comparing whole-track AFD between concussed (blue) and healthy control (red) groups. Horizontal black lines illustrate group medians, the edges of the boxes illustrate 75th (upper edge) and 25th (lower edge) percentiles, vertical black lines illustrate ranges, and black '+' signs illustrate outliers. **b** Line plots showing track profiles for AFD, FW, and FW-corrected FA, RD, and AD. Light red and light blue lines indicate median values of each segment for each individual healthy or concussed subject, respectively. Dark red and dark blue lines indicate instead group medians at each segment. Segment 1 of AD track profile contained three extreme values that prevented a proper illustration of the rest of the track profiles. These values were removed for this figure but were kept in analyses. *$p < 0.05$

Table 4 Results for track 21-179

Segment	Metric	Concussed	Healthy	Mann–Whitney	
				W	*p*
Whole track	AFD	0.1283	0.1371	399	0.046
2	AD	1.8027×10^{-3}	1.8028×10^{-3}	398	0.045
	MD	0.965×10^{-3}	0.963×10^{-3}	610	0.045
	RD	0.546×10^{-3}	0.543×10^{-3}	610	0.045
3	AFD	0.1278	0.1435	385	0.028

Units of AD, MD, RD = mm^2/s. AFD has no units

the final models that had survived corrections for multiple comparisons. Across all models, consistent with the univariate group comparison, participants with mTBI had significantly lower verbal and visual working memory scores after controlling for diffusion metrics. Further, after controlling for the effect of group, diffusion metrics in these models remained significant. As expected, the interaction terms were not significant in any model.

Controlling for repeat mTBIs. The impacts of concussions on the brain can accumulate as more injuries are incurred (Sundman et al. 2015). Three participants in this study had sustained a prior concussion: two had sustained one prior

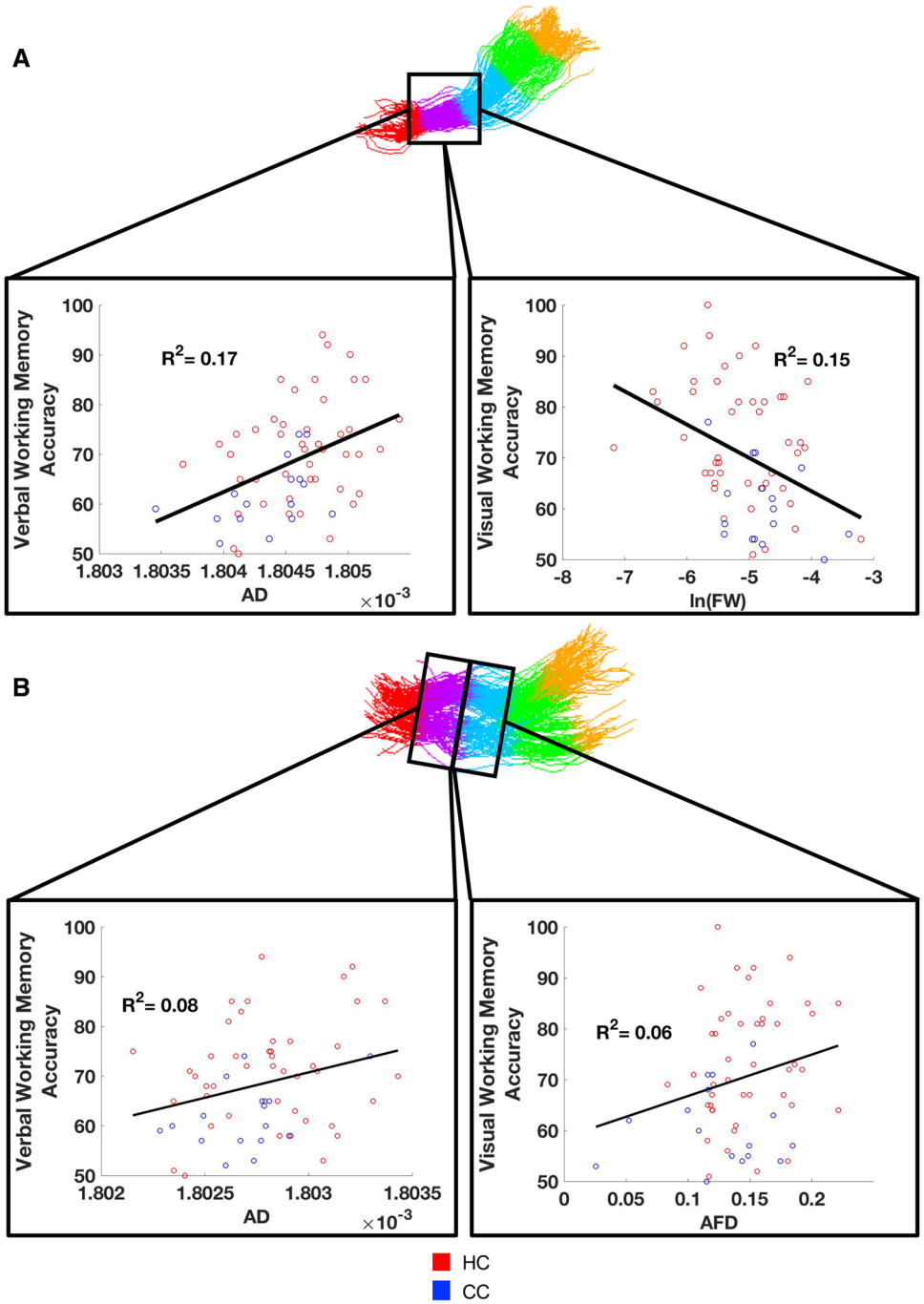

Fig. 6 **a** Correlations between AD and verbal working memory accuracy (left) and the log-transformed FW and visual working memory accuracy (right) in segment 2 of track 16-246. **b** Correlations between AD and verbal working memory accuracy (left) in segment 2 and AFD and visual working memory accuracy (right) in segment 3 of track 21-179

concussion, and one person had sustained six (Table 2). This person also had the highest PCS score. Hence, to account for the impact of prior TBIs, we first excluded this participant and performed Mann–Whitney group comparisons on the diffusion metrics that were included in the final regression models. Except for AFD in segment 2 of track 21-179, all other group differences remained significant. We also reran the final regressions after excluding this participant. All results remained consistent. We then excluded the two additional participants that had a single previous mTBI and repeated these analyses. No results changed, suggesting that the present findings are not driven by repeat mTBIs.

Time since injury. The present study focused on one particular period of concussion neuropathology, the sub-acute period. However, this period has a long time range (Dodd et al. 2014), and hence the time from injury to assessment may still have influenced the present findings. Given that this variable is only relevant for concussed participants, we first reran the final regressions on the concussed group and then added 'time since injury' to the models. No diffusion

Table 5 Correlations between track structure and Post-Concussion Scale (PCS) items

Track	Segment	Metric	PCS item	Correlation	
				r	*p*
16-246	2	AD	Remembering difficulties	− 0.533	0.034
		FW	Vomiting	0.805	< 0.001
			Visual problems	− 0.516	0.041
			Balance	− 0.483	0.058
22-246	2	FA	Nausea	0.611	0.012
			Remembering difficulties	− 0.469	0.067
22-232	2	FA	Nausea	0.593	0.015
			Dizziness	0.522	0.038
21-179	2	AD	Noise sensitivity	− 0.587	0.017
			Remembering difficulties	− 0.493	0.052
		AFD	Sadness	− 0.491	0.053

metrics, before or after the addition of this variable, were significantly related to working memory, and neither was time since injury likely as a result of a lack of power. However, adding time since injury increased the variance accounted by models predicting verbal working memory (average R^2 change = 8.75%), whereas the variance accounted by models predicting visual working memory was not increased (average R^2 change = 1.5%). Further, tolerance, VIF, and condition indices did not suggest the presence of multicollinearity in models that included time since injury. Despite the lack of power, these results suggest that although time since injury is an important predictor for verbal working memory, it is not a confounding variable for diffusion metrics.

Number of fiber orientations. To assess whether changes in FA, AD, MD, and RD of tracks 16-246, 22-246, and 22-232 were due to changes in the number of crossing fiber populations, NuFO values were computed along these tracks. No significant differences were found between groups.

Replication on run 2

To assess the reliability of the present results, analyses that yielded significant group differences with run 1 data were repeated with run 2 data. For the subset of individuals whose second scans passed initial QA ($n = 40$, 10 concussed, 30 controls), we first selected tracks using the same criteria as in run 1. Ten tracks were selected from run 2 scans, only two of which were not within the run 1 tracks. From the four tracks that showed tractometry differences in run 1, three (16-246, 22-232, and 21-179) were among the ten selected from run 2 scans. Only one healthy control did not have a streamline for track 22-246. Nonetheless, only results obtained in tracks 16-246, 22-232, and 21-179 were considered for this replication phase.

In run 2 scans (Table S4), concussed youths had a significantly lower normalized streamline count than healthy controls in track 16-246, a lower AD, and higher MD and RD across track 21-179. In addition, in run 2 scans, concussed youths also had lower AD and higher MD and RD in track 16-246 segment 2, track 22-232 segments 2 and 3, and track 21-179 segment 2. Lastly, concussed youths had lower AFD in segment 3 of track 21-179.

Voxel-overlap scores

On the subset of individuals whose second scans passed initial QA, voxel-overlap scores were computed to assess the reliability of our tractography procedure. FA maps from run 2 scans were converted into run 1 DWI space using ANTs. Overlap scores were computed by assessing the amount of voxels traversed by the same track in both scans, and scores were weighted by track density to minimize the effect of spurious tracks. Across 40 participants, track 16-246 had an average voxel-overlap score of 0.81 (SD = 0.09), track 22-232 an average of 0.85 (SD = 0.08), and track 21-179 an average of 0.66 (SD = 0.16).

Total number of streamlines

The total number of streamlines was variable (SD = 7.58×10^5). Although streamline counts for each track were normalized by total streamline count for each subject, we wanted to ensure that concussed individuals did not have a feature that made tracking globally harder. We thus compared total streamline counts between groups. No significant differences were found (CC: 1.98×10^6, HC: 2.06×10^6; $W = 446$, $p = 0.355$). If fiber tracking is more difficult in concussed individuals, we would also expect reconstructions to be less reliable. Hence, we compared voxel-overlap scores for the three tracks of interest between groups. No significant differences were seen for track 16-246 (CC: 0.793, HC: 0.837; $W = 182$, $p = 0.488$), 22-232 (CC: 0.86, HC: 0.87, $W = 180$, $p = 0.220$), or 21-179 (CC: 0.603, HC: 0.690; $W = 116$, $p = 0.233$).

Discussion

In the present study, we leveraged recent advances in DWI local modeling (CSD, free-water modeling), tractography (PFT with anatomical priors), and tractometry (AFD, FW, FW-corrected tensor measures, and track profiling), to better understand the neuropathological basis of working memory deficits after concussions. After a rigorous, functionally informed, track selection procedure, we identified 11 reliable

working memory tracks. For four of these tracks, we found distinct patterns of microstructural changes, which were correlated to different degrees with working memory performance and with patient-reported memory impairments. Structural differences and tractography reconstructions were reproduced using test–retest analyses.

Interpreting microstructural differences at whole-track and segment levels

At the whole-track level, concussed youths displayed lower streamline count for two thalamo-prefrontal tracks, lower AD, and higher RD and MD for three thalamo-prefrontal tracks and one cingulo-prefrontal track, and lower AFD in the cingulo-prefrontal track. At the segment level, concussed youth also demonstrated lower FA and AD, and higher RD and MD in the same segment of the three thalamo-prefrontal tracks. Animal studies suggest that decreases in FA accompanied by increases in RD and MD are suggestive of alterations in myelin structure (Budde et al. 2011). Further, an animal model of axonal damage and myelin loss in the corpus callosum demonstrated that decreases in AD are specific to axonal loss (Sun et al. 2006). However, DTI analyses in this study were performed in the middle section of the corpus callosum, where fibers are homogeneously oriented. Given that crossing fibers reduce the anisotropy of the overall voxel, we speculate that the link between AD and axonal density should theoretically decrease when the amount of crossing fibers increases. In contrast, AFD can provide information about axonal density along fascicles, which will be less affected by crossing fibers (Raffelt et al. 2012). In the present study, it is unclear whether axonal loss is present in the thalamo-prefrontal tracks, given that AFD and NuFO were not significantly changed (Jones et al. 2013). A study on mouse models of mTBI examined progression of white matter pathology and found a pattern of acute myelin loss at 3 days followed by a pattern of remyelination at 1 week and excessive myelination by 6 weeks (Mierzwa et al. 2015). In a recent study, Spader et al. (2018) used multicomponent-driven equilibrium single-pulse observation of T1 and T2, a quantitative myelin imaging technique, to study 27 collegiate athletes. They found that athletes had higher myelin water fraction (MWF), a measure of myelin content, when compared to healthy controls at 72 h after injury. In addition, concussed athletes had higher MWF after 3 months compared to themselves at 72 h, supporting the interpretation that an active remyelination process takes place in the brain after concussions. The patterns of change observed in the thalamo-prefrontal tracks in concussed youths in the present study are therefore consistent with an altered, possibly excessive and disordered, myelin structure.

In the cingulo-prefrontal track, the patterns of change, which included higher RD and MD, were also suggestive of myelin structure alterations. However, AD and AFD were lower in concussed youths in this track, which is more suggestive of axonal loss. Patterns of tensor-based changes suggestive of axonal loss have been previously observed in studies of concussed individuals (Goswami et al. 2016; Mac Donald et al. 2011). The present study confirms such findings by demonstrating differences in AFD (Raffelt et al. 2012). The presence of potential axonal loss in concussed individuals is important, as these injuries are often believed to be transient (Sharp and Jenkins 2015).

Only one segment of track 16-246 was found to have increased FW in concussed individuals, and this finding was not replicated in run 2 scans. Although edema is an important and well-documented concussive neuropathology (Bigler and Maxwell 2012; Hayes et al. 2016; Werner and Engelhard 2007), the present results suggest that this pathology was not widespread in this particular concussed group. Animal models of TBI suggest that edema is resorbed after 1 week (Bareyre et al. 1997), so perhaps it had been nearly completely resolved in our participants. The group difference in FW reported in the present study was not replicated in test–retest analyses, suggesting that it may possibly be an artifact. This interpretation is also suggested by the paradoxical negative correlations between FW and PCS scores for balance and visual problems. On the other hand, the model using FW to predict visual working memory accounted for 15% of the variance, and FW was highly, positively correlated to the PCS score for vomiting ($r = 0.805$, $p < 0.001$). The interpretation for these results is therefore unclear.

Lastly, based on regression analyses, only measures of the thalamo-prefrontal tracks were significantly related to verbal and visual working memory accuracy. White matter structure in the cingulo-prefrontal track was not related to working memory after correcting for multiple comparisons. These results suggest that neuropathology, in this case suggestive of myelin structure alterations, in thalamo-prefrontal tracks appears to play a key role in working memory deficits in concussion. Consistent with the present results, a recent study performed in mice found that thalamus-to-PFC circuits were important for supporting working memory maintenance (Bolkan et al. 2017). Previous studies have repeatedly found that damage to the thalamus plays an important role in the development of cognitive dysfunctions after mTBIs (Abdel-Dayem et al. 1998; Anderson et al. 1996; Ge et al. 2009; Grossman et al. 2012; Grossman and Inglese 2016; Henninger et al. 2007; Little et al. 2010; Wood and Bigler 1995). Further, in fMRI studies, the thalamus has been repeatedly reported among areas demonstrating abnormal activity in concussed individuals (Chen et al. 2007, 2004; Jantzen et al. 2004; Keightley et al. 2014; McAllister et al. 1999, 2001; Pardini et al. 2010; Westfall et al. 2015). Despite their significance not surviving an FDR correction for

multiple comparisons, it is notable that out of 22 PCS items, symptom scores for remembering difficulties were among the few that were moderately ($r = 0.4$–0.6) correlated with microstructural measurements of the studied tracks. AD in track 21-179 was also negatively correlated with self-reported remembering difficulties ($r = -0.493$, $p = 0.052$), albeit non-significantly (before FDR correction). One potential explanation for this result is that PCS ratings for remembering difficulties may encompass more general memory function than the presently used working memory task.

It is unclear whether these neuropathological findings are generalizable. It is possible that due to demographics or the mechanism of injury in our group (sports injuries), or another unaccounted factor, thalamo-prefrontal tracks may be most affected. However, simulation studies suggest that, given its position near the base of the brain where space is more restricted, the thalamus is among the regions that experiences the highest shear strain from forces transmitted during various forms of head injury mechanisms (Bayly et al. 2005; Sabet et al. 2008; Viano et al. 2005; Zhang et al. 2004). It is therefore possible that these thalamo-frontal tracks tend to be affected across mTBI subjects, irrespective of the mechanism of injury. Factors specific to the present dataset may also possibly explain why the studied thalamo-prefrontal tracks predominantly display a demyelinating profile. Although an imperfect remyelination mechanism may explain why some patients recover from symptoms while others do not, a recent study convincingly showed that in the transneuronal spread of neurodegenerative diseases, axonal loss may always be preceded by myelin alterations, suggesting that neuroinflammation may be playing a role (You et al. 2019). Given the known neuroinflammatory response in concussions, the different neuropathologies observed may instead be parts of a continuum rather than parallel pathologies.

In the present study, we found patterns of change in segments of tracks that were not found at the whole-track level. Across the three thalamo-prefrontal tracks, the same segment, (segment 2 starting from the thalamus) tended to show differences between groups. Two of these tracks shared the same origin in the thalamus and only diverged near the cortex. The other track had a different thalamic origin, but shared the same prefrontal termination as one of the other tracks. Given the proximity of all the tracks, it is possible that the pattern of change arose from damage to a single white matter tract, the thalamic–prefrontal peduncle (Sun et al. 2018). Localized changes in white matter structure can be influenced by the shape of the tract at different segments or the proximity of other structures (Yeatman et al. 2012). Although fiber crossings at different parts of these tracks are an unlikely explanation, it is nonetheless unclear what exact factors contributed to the highly localized changes observed in the present study.

Technical considerations

A recent study applied another novelty of dMRI, the Neurite Orientation Dispersion and Density Imaging (NODDI) model, to study concussions in a sample of individuals aged 18–55 years (Palacios et al. 2018). They found decreases in FA and MD early after injury, as well as elevated free water fraction. They also found longer-term declines in neurite density. The authors attributed the early changes to vasogenic edema and the later changes to neuronal loss. These results also demonstrate the presence of distinct neuropathologies in concussed individuals, although notable differences exist between the two studies. First, Palacios et al. (2018) studied adults, whereas we studied children. This difference is important given that mTBI incidences peak in children and adolescents (Faul et al. 2010), concussed youth have worse outcomes than adults (Hessen et al. 2007; McKinlay et al. 2014), and far fewer biomarker studies exist in children than adults (Mayer et al. 2018). Second, Palacios et al. (2018) used NODDI, whereas we used CSD, novel tractography methods, FW corrections, and track profiling to help refine track segmentation and measurements of white matter microstructure. This difference is important because, despite its advantages over the tensor model, NODDI still assumes a single-fiber population, whereas the methods used presently are more robust to this assumption, especially CSD, which can account for crossing fibers better than NODDI. The addition of more specific measurements of white matter microstructure (FW, NuFO, AFD) helped complement the information provided by tensor measures. Nonetheless, these tensor-based measurements, similar to NODDI-derived metrics, remain voxel-level measurements and thus not tract specific. Instead, CSD gives rise to fODFs and fiber elements (or "fixels") (Raffelt et al. 2017) which can provide intra-voxel, orientation-dependent fiber density information along fiber fascicles. Although more research is needed to compare AFD against NODDI metrics in terms of neuropathological information, AFD computed along "fixels" provides measurements that are more tract specific.

Clinical considerations

Although no universal consensus exists for the definition of a biomarker, prior work suggests that a clinically useful biomarker needs to reliably and objectively detect the presence or absence of disease, track the rate of disease progression, and provide information on the mechanism of disease and clinical outcome to inform the most appropriate course of therapy (Holland 2016; Salter and Holland 2014). This last criterion is often overlooked in concussions. Although

reviews and DTI studies have proposed that FA can serve as a concussion biomarker (Churchill et al. 2017; Hulkower et al. 2013), given the limitations of the tensor model, FA lacks specificity and therefore cannot provide information on the disease process (Dodd et al. 2014; Jones et al. 2013). Despite using novel, more neuropathologically informative tools, no particular biomarker appeared to emerge in this study, as different metrics were identified in different analyses. These findings are consistent with reviews and studies demonstrating the extensive heterogeneity of concussion neuropathology (Bigler and Maxwell 2012; Dodd et al. 2014; Ware et al. 2017) and the low specificity of most dMRI metrics (Jones et al. 2013). Another important observation is the low effect size of the white matter changes reported in the present study. Concussions are known to be subtle, and replication studies are needed to assess whether these small differences in white matter structure can be reliably detected.

Implications for future research

Our findings add to previous literature implicating the thalamus and the DLPFC in working memory, and provide a set of tracks of interest for future studies of working memory deficits in concussion. Further, this study used a symptom-driven track-of-interest selection, by finding tracks connecting ROIs that are related to the symptom of interest. Although the present study used group comparisons, future research needs to explore this symptom-driven track-of-interest selection approach further, using other symptoms, to assess whether a fully individualized, symptom-driven approach offers an advantage over the classical, whole-brain, group-comparison design. Nonetheless, the track selection procedure introduced in this study contributes to a growing literature that is moving away from simplistic group-comparison studies that treat all concussions as being the same, and use tensor metrics—often a single one—to find concussion biomarkers.

Limitations and strengths

First, groups were not balanced for handedness. In a study of 42 right and 40 left handers aged 18–31 years, Powell et al. (2012) used voxel-based statistics and found that self-reported right handers had higher FA in the left hemisphere's limbic cortex, PFC, medial frontal lobe, and inferior frontal gyrus, and the right hemisphere's orbitofrontal cortex, and middle and inferior frontal gyri. It is possible that our concussed group, which contained significantly more left handers, had lower FA than healthy controls because of handedness rather than injury. Powell et al. (2012) correctly argue that their results depend on an assumption of similar numbers of crossing fibers between left and right handers. No conclusive evidence exists to support this assumption, and the present study, by using new methods that can provide orientation-specific information that is robust to underlying fiber configuration, can overcome the potentially confounding factors that may be present in the Powell et al. (2012) study. Second, the sample size was relatively small for the number of tests performed, raising concerns about insufficiency of power. Several efforts were taken to limit the number of tests, which, when using track profiling, could have been exponentially greater, but as a consequence, other important differences may have been missed. Replication with larger datasets is necessary. Despite recruiting participants within the sub-acute period of concussion, the interval from injury to testing was variable. A larger dataset is therefore also necessary to model the effects of a highly variable post-concussion interval. Third, although the neuropathological interpretations advanced in this study are supported by previous and recent literature, these techniques do not offer the same level of specificity as other forms of microstructural imaging. Replication with other modalities, especially with myelin-based contrast imaging, and validation with histological studies are therefore still needed. Lastly, the cross-sectional design of this study prevents inferences on clinical outcomes. Future longitudinal studies of concussed children are needed to assess whether patterns of change suggesting different types of neuropathologies are associated with different clinical outcomes.

In addition to using novel methodology, the strengths of the present study include the use of a sample of age- and sex-matched controls, a high-angular resolution dataset to ensure rotationally invariant tensor (Jones 2004) and fODF reconstructions (Jones et al. 2013), and a strict QA procedure. Further, the use of strict track selection criteria ensured that tractometry analyses were performed only on a reliable set of tracks. The tracks with the majority of effects, 16-246, 22-232, and 21-179, were reconstructed across all 102 selected scans, making these tracks highly replicable. Voxel-overlap scores between run 1 and run 2 tracks also reflect this high reliability. Although the average voxel-overlap score in track 21-179 was lower than that in track 16-246, its standard deviation was larger, suggesting that this track may be harder to reconstruct, perhaps due to its particular anatomical location and proximity to major white matter bundles (Figure S2). Results on this track were replicated on run 2 data, despite the higher difficulty associated with its reconstruction. Lastly, the use of PCS scores provided a way to validate the clinical relevance of track measurements.

Conclusion

This study applied major recent advances in dMRI to better understand the neuropathology involved in working memory deficits in sub-acutely concussed youths. The present

results suggest that myelin structure alterations in thalamo-prefrontal tracks play a key role in working memory impairments after concussions. More broadly, this study observed patterns suggesting the presence of concurrent pathologies in the brains of concussed children. Neuropathologically informed, clinically useful biomarkers are still needed, and by providing a better understanding of the neuropathology involved in sub-acute pediatric concussions, the present study provides a basis for future research aiming to develop concussion biomarkers.

Acknowledgements We want to thank the participants and their parents for lending their time for this study. We also want to thank Dr. Jen-Kai Chen and Dr. Rajeet Singh Salujah for their contribution in the acquisition of this data.

Funding Funding for this study came from: 1. a Vanier Canada Graduate Research award, the Fonds de Recherche du Quebec—Doctoral Training for Medical Students award, and the Tomlinson Doctoral Fellowship award (G. I. Guberman); 2. an Institutional Research Chair in Neuroinformatics and National Science and Engineering Research Council Discovery Grants (Dr. Descoteaux); 3. a Canadian Institutes of Health Research Grant (Dr. Ptito, Dr. Gagnon); 4. A Fonds de Recherche du Quebec senior clinical research scholar award, and support from the Research Institute of the McGill University Health Centre (Dr. Gagnon).

Compliance with ethical standards

Conflict of interest The authors have no conflicts of interest to declare.

Ethics approval Every participant provided informed written consent as approved by the ethics committee at McGill University, Montreal Neurological Institute.

References

Abdel-Dayem HM, Abu-Judeh H, Kumar M, Atay S, Naddaf S, El-Zeftawy H, Luo JQ (1998) SPECT brain perfusion abnormalities in mild or moderate traumatic brain injury. Clin Nucl Med 23:309–317

Anderson CV, Wood DM, Bigler ED, Blatter DD (1996) Lesion volume, injury severity, and thalamic integrity following head injury. J Neurotrauma 13:59–65. https://doi.org/10.1089/neu.1996.13.59

Andersson JLR, Sotiropoulos SN (2016) An integrated approach to correction for off-resonance effects and subject movement in diffusion MR imaging. Neuroimage 125:1063–1078. https://doi.org/10.1016/j.neuroimage.2015.10.019

Avants BB, Epstein CL, Grossman M, Gee JC (2008) Symmetric diffeomorphic image registration with cross-correlation: evaluating automated labeling of elderly and neurodegenerative brain. Med Image Anal 12:26–41. https://doi.org/10.1016/j.media.2007.06.004

Avants BB, Tustison NJ, Song G, Cook PA, Klein A, Gee JC (2011) A reproducible evaluation of ANTs similarity metric performance in brain image registration. Neuroimage 54:2033–2044. https://doi.org/10.1016/j.neuroimage.2010.09.025

Bareyre F, Wahl F, McIntosh TK, Stutzmann JM (1997) Time course of cerebral edema after traumatic brain injury in rats: effects of riluzole and mannitol. J Neurotrauma 14:839–849. https://doi.org/10.1089/neu.1997.14.839

Bayly PV, Cohen TS, Leister EP, Ajo D, Leuthardt EC, Genin GM (2005) Deformation of the human brain induced by mild acceleration. J Neurotrauma 22:845–856. https://doi.org/10.1089/neu.2005.22.845

Bigler ED, Maxwell WL (2012) Neuropathology of mild traumatic brain injury: relationship to neuroimaging findings. Brain Imaging Behav 6:108–136. https://doi.org/10.1007/s11682-011-9145-0

Bolkan SS et al (2017) Thalamic projections sustain prefrontal activity during working memory maintenance. Nat Neurosci 20:987–996. https://doi.org/10.1038/nn.4568

Budde MD, Janes L, Gold E, Turtzo LC, Frank JA (2011) The contribution of gliosis to diffusion tensor anisotropy and tractography following traumatic brain injury: validation in the rat using Fourier analysis of stained tissue sections. Brain 134:2248–2260. https://doi.org/10.1093/brain/awr161

Carroll LJ et al (2004) Prognosis for mild traumatic brain injury: results of the WHO Collaborating Centre Task Force on Mild Traumatic Brain Injury. J Rehabil Med (43 Suppl):84–105

Cassidy JD et al (2004) Incidence, risk factors and prevention of mild traumatic brain injury: results of the WHO Collaborating Centre Task Force on Mild Traumatic Brain Injury. J Rehabil Med (43 Suppl):28–60

Chen JK, Johnston KM, Frey S, Petrides M, Worsley K, Ptito A (2004) Functional abnormalities in symptomatic concussed athletes: an fMRI study. Neuroimage 22:68–82. https://doi.org/10.1016/j.neuroimage.2003.12.032

Chen JK, Johnston KM, Collie A, McCrory P, Ptito A (2007) A validation of the post concussion symptom scale in the assessment of complex concussion using cognitive testing and functional MRI. J Neurol Neurosurg Psychiatry 78:1231–1238. https://doi.org/10.1136/jnnp.2006.110395

Churchill NW, Hutchison MG, Richards D, Leung G, Graham SJ, Schweizer TA (2017) Neuroimaging of sport concussion: persistent alterations in brain structure and function at medical clearance. Sci Rep 7:8297. https://doi.org/10.1038/s41598-017-07742-3

Daducci A, Canales-Rodriguez EJ, Zhang H, Dyrby TB, Alexander DC, Thiran JP (2015) Accelerated microstructure imaging via convex optimization (AMICO) from diffusion MRI data. Neuroimage 105:32–44. https://doi.org/10.1016/j.neuroimage.2014.10.026

Dean PJ, O'Neill D, Sterr A (2012) Post-concussion syndrome: prevalence after mild traumatic brain injury in comparison with a sample without head injury. Brain Inj 26:14–26. https://doi.org/10.3109/02699052.2011.635354

Dell'Acqua F, Simmons A, Williams SC, Catani M (2013) Can spherical deconvolution provide more information than fiber orientations? Hindrance modulated orientational anisotropy, a true-tract specific index to characterize white matter diffusion. Hum Brain Mapp 34:2464–2483. https://doi.org/10.1002/hbm.22080

Descoteaux M, Deriche R, Knosche TR, Anwander A (2009) Deterministic and probabilistic tractography based on complex fibre orientation distributions. IEEE Trans Med Imaging 28:269–286. https://doi.org/10.1109/TMI.2008.2004424

Dodd AB, Epstein K, Ling JM, Mayer AR (2014) Diffusion tensor imaging findings in semi-acute mild traumatic brain injury. J Neurotrauma 31:1235–1248. https://doi.org/10.1089/neu.2014.3337

Douaud G et al (2011) DTI measures in crossing-fibre areas: increased diffusion anisotropy reveals early white matter alteration in MCI and mild Alzheimer's disease. Neuroimage 55:880–890. https://doi.org/10.1016/j.neuroimage.2010.12.008

Dyrby TB, Lundell H, Burke MW, Reislev NL, Paulson OB, Ptito M, Siebner HR (2014) Interpolation of diffusion weighted imaging datasets. Neuroimage 103:202–213. https://doi.org/10.1016/j.neuroimage.2014.09.005

Fan L et al (2016) the human brainnetome atlas: a new brain atlas based on connectional architecture. Cereb Cortex 26:3508–3526. https://doi.org/10.1093/cercor/bhw157

Faul M, Xu L, Wald M, Coronado V (2010) Traumatic brain injury in the United States: emergency department visits, hospitalizations, and deaths. Centers for Disease Control and Prevention National Center for Injury Prevention and Control, Atlanta

Garyfallidis E et al (2014) Dipy, a library for the analysis of diffusion MRI data. Front Neuroinform 8:8. https://doi.org/10.3389/fninf.2014.00008

Ge Y et al (2009) Assessment of thalamic perfusion in patients with mild traumatic brain injury by true FISP arterial spin labelling MR imaging at 3T. Brain Inj 23:666–674. https://doi.org/10.1080/02699050903014899

Girard G, Whittingstall K, Deriche R, Descoteaux M (2014) Towards quantitative connectivity analysis: reducing tractography biases. Neuroimage 98:266–278. https://doi.org/10.1016/j.neuroimage.2014.04.074

Goswami R et al (2016) Frontotemporal correlates of impulsivity and machine learning in retired professional athletes with a history of multiple concussions. Brain Struct Funct 221:1911–1925. https://doi.org/10.1007/s00429-015-1012-0

Grossman EJ, Inglese M (2016) The role of thalamic damage in mild traumatic brain injury. J Neurotrauma 33:163–167. https://doi.org/10.1089/neu.2015.3965

Grossman EJ et al (2012) Thalamus and cognitive impairment in mild traumatic brain injury: a diffusional kurtosis imaging study. J Neurotrauma 29:2318–2327. https://doi.org/10.1089/neu.2011.1763

Guberman G (2019) Montreal Neurological Institute—pediatric concussion. https://doi.org/10.17605/OSF.IO/QKVS7

Harsan LA et al (2006) Brain dysmyelination and recovery assessment by noninvasive in vivo diffusion tensor magnetic resonance imaging. J Neurosci Res 83:392–402. https://doi.org/10.1002/jnr.20742

Hayes JP, Bigler ED, Verfaellie M (2016) Traumatic brain injury as a disorder of brain connectivity. J Int Neuropsychol Soc 22:120–137. https://doi.org/10.1017/S1355617715000740

Henninger N et al (2007) Differential recovery of behavioral status and brain function assessed with functional magnetic resonance imaging after mild traumatic brain injury in the rat. Crit Care Med 35:2607–2614. https://doi.org/10.1097/01.CCM.0000286395.79654.8D

Hessen E, Nestvold K, Anderson V (2007) Neuropsychological function 23 years after mild traumatic brain injury: a comparison of outcome after paediatric and adult head injuries. Brain Inj 21:963–979. https://doi.org/10.1080/02699050701528454

Holland RL (2016) What makes a good biomarker? Adv Precis Med 1:66–77

Hulkower MB, Poliak DB, Rosenbaum SB, Zimmerman ME, Lipton ML (2013) A decade of DTI in traumatic brain injury: 10 years and 100 articles later. Am J Neuroradiol 34:2064–2074. https://doi.org/10.3174/ajnr.A3395

Jantzen KJ, Anderson B, Steinberg FL, Kelso JA (2004) A prospective functional MR imaging study of mild traumatic brain injury in college football players. Am J Neuroradiol 25:738–745

Jeurissen B, Leemans A, Tournier JD, Jones DK, Sijbers J (2013) Investigating the prevalence of complex fiber configurations in white matter tissue with diffusion magnetic resonance imaging. Hum Brain Mapp 34:2747–2766. https://doi.org/10.1002/hbm.22099

Jones DK (2004) The effect of gradient sampling schemes on measures derived from diffusion tensor MRI: a Monte Carlo study. Magn Reson Med 51:807–815. https://doi.org/10.1002/mrm.20033

Jones DK, Knosche TR, Turner R (2013) White matter integrity, fiber count, and other fallacies: the do's and don'ts of diffusion MRI. Neuroimage 73:239–254. https://doi.org/10.1016/j.neuroimage.2012.06.081

Keightley ML, Saluja RS, Chen JK, Gagnon I, Leonard G, Petrides M, Ptito A (2014) A functional magnetic resonance imaging study of working memory in youth after sports-related concussion: is it still working? J Neurotrauma 31:437–451. https://doi.org/10.1089/neu.2013.3052

Kristman VL et al (2014) Methodological issues and research recommendations for prognosis after mild traumatic brain injury: results of the International Collaboration on Mild Traumatic Brain Injury Prognosis. Arch Phys Med Rehabil 95:S265–277. https://doi.org/10.1016/j.apmr.2013.04.026

Landre N, Poppe CJ, Davis N, Schmaus B, Hobbs SE (2006) Cognitive functioning and postconcussive symptoms in trauma patients with and without mild TBI. Arch Clin Neuropsychol 21:255–273. https://doi.org/10.1016/j.acn.2005.12.007

Lewine JD, Davis JT, Sloan JH, Kodituwakku PW, Orrison WW Jr (1999) Neuromagnetic assessment of pathophysiologic brain activity induced by minor head trauma. Am J Neuroradiol 20:857–866

Little DM et al (2010) Thalamic integrity underlies executive dysfunction in traumatic brain injury. Neurology 74:558–564. https://doi.org/10.1212/WNL.0b013e3181cff5d5

Lovell MR et al (2006) Measurement of symptoms following sports-related concussion: reliability and normative data for the post-concussion scale. Appl Neuropsychol 13:166–174. https://doi.org/10.1207/s15324826an1303_4

Mac Donald CL et al (2011) Detection of blast-related traumatic brain injury in U.S. military personnel. N Engl J Med 364:2091–2100. https://doi.org/10.1056/NEJMoa1008069

Mac Donald CL, Dikranian K, Bayly P, Holtzman D, Brody D (2007) Diffusion tensor imaging reliably detects experimental traumatic axonal injury and indicates approximate time of injury. J Neurosci 27:11869–11876. https://doi.org/10.1523/JNEUROSCI.3647-07.2007

Maintz JA, Viergever MA (1998) A survey of medical image registration. Med Image Anal 2:1–36

Mayer AR et al (2018) Advanced biomarkers of pediatric mild traumatic brain injury: progress and perils. Neurosci Biobehav Rev. https://doi.org/10.1016/j.neubiorev.2018.08.002

McAllister TW et al (1999) Brain activation during working memory 1 month after mild traumatic brain injury: a functional MRI study. Neurology 53:1300–1308

McAllister TW, Sparling MB, Flashman LA, Guerin SJ, Mamourian AC, Saykin AJ (2001) Differential working memory load effects after mild traumatic brain injury. Neuroimage 14:1004–1012. https://doi.org/10.1006/nimg.2001.0899

McKee AC et al (2009) Chronic traumatic encephalopathy in athletes: progressive tauopathy after repetitive head injury. J Neuropathol Exp Neurol 68:709–735

McKinlay A, Corrigan J, Horwood LJ, Fergusson DM (2014) Substance abuse and criminal activities following traumatic brain injury in childhood, adolescence, and early adulthood. J Head Trauma Rehabil 29:498–506. https://doi.org/10.1097/HTR.0000000000000001

Meehan WP 3rd, Mannix RC, O'Brien MJ, Collins MW (2013) The prevalence of undiagnosed concussions in athletes. Clin J Sport Med 23:339–342. https://doi.org/10.1097/JSM.0b013e318291d3b3

Mierzwa AJ, Marion CM, Sullivan GM, McDaniel DP, Armstrong RC (2015) Components of myelin damage and repair in the progression of white matter pathology after mild traumatic brain injury. J Neuropathol Exp Neurol 74:218–232. https://doi.org/10.1097/NEN.0000000000000165

Mito R et al (2018) Fibre-specific white matter reductions in Alzheimer's disease and mild cognitive impairment. Brain. https://doi.org/10.1093/brain/awx355

Orlovska S, Pedersen MS, Benros ME, Mortensen PB, Agerbo E, Nordentoft M (2014) Head injury as risk factor for psychiatric disorders: a nationwide register-based follow-up study of 113,906 persons with head injury. Am J Psychiatry 171:463–469

Palacios E et al (2018) The evolution of white matter changes after mild traumatic brain injury: a DTI and NODDI study. bioRxiv. https://doi.org/10.1101/345629

Pardini JE, Pardini DA, Becker JT, Dunfee KL, Eddy WF, Lovell MR, Welling JS (2010) Postconcussive symptoms are associated with compensatory cortical recruitment during a working memory task. Neurosurgery 67:1020–1027. https://doi.org/10.1227/NEU.0b013e3181ee33e2**(discussion 1027–1028)**

Pasternak O, Sochen N, Gur Y, Intrator N, Assaf Y (2009) Free water elimination and mapping from diffusion MRI. Magn Reson Med 62:717–730. https://doi.org/10.1002/mrm.22055

Pasternak O, Shenton ME, Westin CF (2012) Estimation of extracellular volume from regularized multi-shell diffusion MRI. Med Image Comput Comput Assist Interv 15:305–312

Pasternak O, Kubicki M, Shenton ME (2016) vivo imaging of neuroinflammation in schizophrenia. Schizophr Res 173:200–212. https://doi.org/10.1016/j.schres.2015.05.034

Peeters W, van den Brande R, Polinder S, Brazinova A, Steyerberg EW, Lingsma HF, Maas AI (2015) Epidemiology of traumatic brain injury in Europe. Acta Neurochir (Wien) 157:1683–1696. https://doi.org/10.1007/s00701-015-2512-7

Petrides M, Alivisatos B, Meyer E, Evans AC (1993) Functional activation of the human frontal cortex during the performance of verbal working memory tasks. Proc Natl Acad Sci USA 90:878–882

Petrides M, Frey S, Chen J-K (2001) Increased activation of the mid-dorsolateral frontal cortex during the monitoring of abstract visual and verbal stimuli. Neuroimage 6:721

Pierpaoli C, Basser PJ (1996) Toward a quantitative assessment of diffusion anisotropy. Magn Reson Med 36:893–906

Pierpaoli C, Barnett A, Pajevic S, Chen R, Penix LR, Virta A, Basser P (2001) Water diffusion changes in Wallerian degeneration and their dependence on white matter architecture. Neuroimage 13:1174–1185. https://doi.org/10.1006/nimg.2001.0765

Powell JL, Parkes L, Kemp GJ, Sluming V, Barrick TR, Garcia-Finana M (2012) The effect of sex and handedness on white matter anisotropy: a diffusion tensor magnetic resonance imaging study. Neuroscience 207:227–242. https://doi.org/10.1016/j.neuroscience.2012.01.016

Raffelt DA et al (2012) Apparent Fibre Density: a novel measure for the analysis of diffusion-weighted magnetic resonance images. Neuroimage 59:3976–3994. https://doi.org/10.1016/j.neuroimage.2011.10.045

Raffelt DA, Tournier JD, Smith RE, Vaughan DN, Jackson G, Ridgway GR, Connelly A (2017) Investigating white matter fibre density and morphology using fixel-based analysis. Neuroimage 144:58–73. https://doi.org/10.1016/j.neuroimage.2016.09.029

Sabet AA, Christoforou E, Zatlin B, Genin GM, Bayly PV (2008) Deformation of the human brain induced by mild angular head acceleration. J Biomech 41:307–315. https://doi.org/10.1016/j.jbiomech.2007.09.016

Salter H, Holland R (2014) Biomarkers: refining diagnosis and expediting drug development—reality, aspiration and the role of open innovation. J Intern Med 276:215–228. https://doi.org/10.1111/joim.12234

Sharp DJ, Jenkins PO (2015) Concussion is confusing us all. Pract Neurol 15:172–186. https://doi.org/10.1136/practneurol-2015-001087

Shenton ME et al (2012) A review of magnetic resonance imaging and diffusion tensor imaging findings in mild traumatic brain injury. Brain Imaging Behav 6:137–192. https://doi.org/10.1007/s11682-012-9156-5

Smith SM (2002) Fast robust automated brain extraction. Hum Brain Mapp 17:143–155. https://doi.org/10.1002/hbm.10062

Spader HS et al (2018) Prospective study of myelin water fraction changes after mild traumatic brain injury in collegiate contact sports. J Neurosurg. https://doi.org/10.3171/2017.12.JNS171597

Spinos P, Sakellaropoulos G, Georgiopoulos M, Stavridi K, Apostolopoulou K, Ellul J, Constantoyannis C (2010) Postconcussion syndrome after mild traumatic brain injury in Western Greece. J Trauma 69:789–794. https://doi.org/10.1097/TA.0b013e3181edea67

Stern CE, Owen AM, Tracey I, Look RB, Rosen BR, Petrides M (2000) Activity in ventrolateral and mid-dorsolateral prefrontal cortex during nonspatial visual working memory processing: evidence from functional magnetic resonance imaging. Neuroimage 11:392–399. https://doi.org/10.1006/nimg.2000.0569

St-Jean S, Coupe P, Descoteaux M (2016) Non local spatial and angular matching: enabling higher spatial resolution diffusion MRI datasets through adaptive denoising. Med Image Anal 32:115–130. https://doi.org/10.1016/j.media.2016.02.010

Sun SW, Liang HF, Trinkaus K, Cross AH, Armstrong RC, Song SK (2006) Noninvasive detection of cuprizone induced axonal damage and demyelination in the mouse corpus callosum. Magn Reson Med 55:302–308. https://doi.org/10.1002/mrm.20774

Sun C, Wang Y, Cui R, Wu C, Li X, Bao Y, Wang Y (2018) Human thalamic-prefrontal peduncle connectivity revealed by diffusion spectrum imaging fiber tracking. Front Neuroanat 12:24. https://doi.org/10.3389/fnana.2018.00024

Sundman M, Doraiswamy PM, Morey RA (2015) Neuroimaging assessment of early and late neurobiological sequelae of traumatic brain injury: implications for CTE. Front Neurosci 9:334. https://doi.org/10.3389/fnins.2015.00334

Tournier JD, Calamante F, Connelly A (2007) Robust determination of the fibre orientation distribution in diffusion MRI: non-negativity constrained super-resolved spherical deconvolution. Neuroimage 35:1459–1472. https://doi.org/10.1016/j.neuroimage.2007.02.016

Tournier JD, Yeh CH, Calamante F, Cho KH, Connelly A, Lin CP (2008) Resolving crossing fibres using constrained spherical deconvolution: validation using diffusion-weighted imaging phantom data. Neuroimage 42:617–625. https://doi.org/10.1016/j.neuroimage.2008.05.002

Tournier JD, Mori S, Leemans A (2011) Diffusion tensor imaging and beyond. Magn Reson Med 65:1532–1556. https://doi.org/10.1002/mrm.22924

Tournier JD, Calamante F, Connelly A (2012) MRtrix: diffusion tractography in crossing fiber regions. Int J Imaging Syst Technol 22:53–66

Viano DC, Casson IR, Pellman EJ, Zhang L, King AI, Yang KH (2005) Concussion in professional football: brain responses by finite element analysis: part 9. Neurosurgery 57:891–916 **(discussion 891–916)**

Ware JB, Hart T, Whyte J, Rabinowitz A, Detre JA, Kim J (2017) Inter-subject variability of axonal injury in diffuse traumatic brain injury. J Neurotrauma 34:2243–2253. https://doi.org/10.1089/neu.2016.4817

Werner C, Engelhard K (2007) Pathophysiology of traumatic brain injury. Br J Anaesth 99:4–9. https://doi.org/10.1093/bja/aem131

Westfall DR, West JD, Bailey JN, Arnold TW, Kersey PA, Saykin AJ, McDonald BC (2015) Increased brain activation during working memory processing after pediatric mild traumatic brain injury (mTBI). J Pediatr Rehabil Med 8:297–308. https://doi.org/10.3233/PRM-150348

Wood DM, Bigler ED (1995) Diencephalic changes in traumatic brain injury: relationship to sensory perceptual function. Brain Res Bull 38:545–549

Woolrich MW et al (2009) Bayesian analysis of neuroimaging data in FSL. Neuroimage 45:S173–S186. https://doi.org/10.1016/j.neuroimage.2008.10.055

Yeatman JD, Dougherty RF, Myall NJ, Wandell BA, Feldman HM (2012) Tract profiles of white matter properties: automating fiber-tract quantification. PLoS ONE 7:e49790. https://doi.org/10.1371/journal.pone.0049790

You Y et al (2019) Demyelination precedes axonal loss in the transneuronal spread of human neurodegenerative disease. Brain 142:426–442. https://doi.org/10.1093/brain/awy338

Yuh EL et al (2013) Magnetic resonance imaging improves 3-month outcome prediction in mild traumatic brain injury. Ann Neurol 73:224–235. https://doi.org/10.1002/ana.23783

Zhang Y, Brady M, Smith S (2001) Segmentation of brain MR images through a hidden Markov random field model and the expectation-maximization algorithm. IEEE Trans Med Imaging 20:45–57. https://doi.org/10.1109/42.906424

Zhang L, Yang KH, King AI (2004) A proposed injury threshold for mild traumatic brain injury. J Biomech Eng 126:226–236